IEEE Access
Multidisciplinary | Rapid Review | Open Access Journal

Received 18 April 2023, accepted 17 May 2023, date of publication 23 May 2023, date of current version 1 June 2023.

Digital Object Identifier 10.1109/ACCESS.2023.3278800

RESEARCH ARTICLE

Automated Explainable Detection of Cyclic Alternating Pattern (CAP) Phases and Sub-Phases Using Wavelet-Based Single-Channel EEG Signals

MANISH SHARMA[1], HARSH LODHI[1], RISHITA YADAV[1], NIRANJANA SAMPATHILA[2], (Senior Member, IEEE), K. S. SWATHI[3], AND U. RAJENDRA ACHARYA[4]

[1]Department of Electrical and Computer Science Engineering, Institute of Infrastructure, Technology, Research and Management (IITRAM), Ahmedabad 380026, India
[2]Department of Biomedical Engineering, Manipal Institute of Technology, Manipal Academy of Higher Education (MAHE), Manipal 576104, India
[3]Prasanna School of Public Health, Manipal Academy of Higher Education (MAHE), Manipal 576104, India
[4]School of Mathematics, Physics and Computing, University of Southern Queensland, Springfield Central, QLD 4300, Australia

Corresponding author: Niranjana Sampathila (niranjana.s@manipal.edu)

ABSTRACT Sleep is a crucial component of health and well-being. It maintains the metabolism of the body and covers one-third of total life. The assessment of sleep quality is typically done by evaluating the macrostructure-based sleep stages, however, it does not take into account transient phenomena like K-complexes and transient fluctuations, which are crucial for the diagnosis of various sleep disorders. Cyclic alternating pattern (CAP) is a recurrent physiological electroencephalogram (EEG) activity that takes place in the brain during sleep and it is considered as a microstructure of sleep that can provide more accurate and relevant evaluation of sleep. The traditional way of CAP phase division is done manually by sleep specialists, which is sensitive, time-consuming, and prone to inaccuracies. Hence, there is a need for automated detection techniques that can solve the problems. This study proposes an automated, computerized approach for developing a machine learning model with explainable artificial intelligence (XAI) capabilities, using wavelet-based Hjorth parameters for classifying CAP A & B phases and phases A sub-phases (A1, A2, A3). The study utilizes SHAP (SHapley Additive exPlanations)-based feature ranking to provide insights into the model. This study uses the publicly accessible Physionet CAP sleep database. The model is developed using single-channel standardized EEG recordings from healthy subjects and patients with five types of sleep disorders, namely, insomnia, nocturnal frontal lobe epilepsy (NFLE), periodic leg movement disorder (PLM), rapid eye movement behavior disorder (RBD) and narcolepsy. The best performance is obtained using k-nearest neighbors (KNN) and ensemble bagged trees (EbagT) classifiers. The proposed model achieved a average classification accuracy of 91.6% for healthy subjects and 94.33%, 86.3%, 88.68%, 84.43%, and 88.5% for narcolepsy, RBD, PLM, NFLE, and insomnia subjects respectively, for classifying phases A and B. Our model achieved a average classification accuracy of 92.85% for healthy subjects and 93.9%, 84.9%, 88.0%, 80.92%, and 89.41% for narcolepsy, RBD, PLM, NFLE, and insomnia subjects, respectively while categorizing A subphases (A1, A2, A3). The proposed method may help sleep experts to examine a person's sleep quality automatically using the microstructure of sleep.

INDEX TERMS Cyclic alternating patterns (CAP), machine learning, electroencephalogram (EEG), phase A and phase B detection, k-nearest neighbor (kNN), sleep disorders.

The associate editor coordinating the review of this manuscript and approving it for publication was Paolo Crippa.

I. INTRODUCTION

A good night's sleep is essential for the healthy human body and optimum functioning [1]. According to a recent study poor interrupted sleep and sleep disorders all impact various aspects of human health [1]. Every person's mental and physical health unquestionably depends on the quality of sleep they receive [1]. Inadequate sleep may cause blood sugar levels to rise to the point where a person becomes diabetic. Improper sleep may also contribute to coronary artery blockage, resulting in congestive heart failure, stroke, and cardiovascular disease [2]. Inadequate sleep may lower one's quality of life and reduce a person's life span [2]. Proper sleep also aids in the re-calibration of our emotional neural pathways, allowing us to better organize our daily activities and deal with psychological obstacles [2]. During sleep, the brain is doused with neurochemicals, which helps in the consolidation of memories and the formation of a virtual reality environment where past and current experiences and information are integrated [2]. Recent sleep studies have shown that quality sleep is the most effective daily activity for rejuvenating both our brain and body health [2].

As sleep is the most important physiological process of human life, hence the sleep quality assessment is vital. The conventional way of sleep quality assessment is done using the Pittsburgh sleep quality index (PSQI) [3]. PSQI evaluates sleep quality using a self-report questionnaire over a one-month period, including items related to the empirical aspects of sleep quality. In the PSQI survey, the questions are often asked based on sleep duration, snoring during sleep, breathing issues while sleeping, daytime tiredness, caffeine consumption, body-to-mass ratio index, and blood pressure. Their responses are extremely subjective and memory-based, leaving them vulnerable to human error. Maintaining a sleep record or sleep journal for the prior 15 or 30 days is also part of the diagnostic method. The type of sleep disturbance is determined by the physician based on the patient's replies to sleep questionnaires and the information recorded in the sleep diary. However, polysomnography (PSG) is now frequently used to identify sleep problems [4].

In PSG, physiological changes that occur during sleep are recorded by a sleep specialist. It is usually done at night, and complete night sleep is recorded [5]. PSG techniques involve many electrodes and connected sensors to record several physiological signals such as electroencephalogram (EEG) for brain waves, electrocardiogram (ECG) for heart rhythms [6], electromyogram (EMG) for muscle movements, electrooculogram (EOG) for eye movement, thermistors for nasal airflow and blood oxygen saturation (SpO2). Use of many sensors, electrodes, and complexity, the PSG method is expensive, time-consuming, and difficult for patients and potentially problematic for doctors. For the scoring of polysomnographic recordings, a qualified sleep specialist is needed. Furthermore, the procedure is not only time-consuming, but it also poses a significant risk of inaccuracies due to human error. One of the most effective solutions to this problem of scoring is the use of automatic computerized sleep analysis, which has the potential to greatly reduce the chances of errors and increase efficiency.

Sleep is made up of non-rapid eye movement (NREM) stages, in which a person is unconscious, and rapid eye movement (REM) stages, during which there is high brain activity [7]. Initially, according to Rechtschaffen and Kales (R&K) rules [8] there are six stages of sleep, namely: Wakefulness (W), Non-Rapid Eye Movement (NREM), which is subdivided into four stages of sleep (S1, S2, S3, and S4), and Rapid Eye Movement (REM) stage. Later the new guidelines for sleep scoring were provided by the American Academy of Sleep Medicine (AASM) [9]. In this, due to similarities in features of S3 and S4, they are referred to as slow wave sleep (SWS) or N3 sleep stage. Hence, effectively five sleep stages are there: W, NREM (N1, N2, N3), and REM. N1 and N2 sleep stages are referred to as light sleep, whereas the N3 sleep stage is referred to as deep sleep [10]. The sleep macrostructure comprises the W, NREM, and REM phases. There are numerous studies in the literature on the macrostructure of sleep based sleep scoring, and researchers have built various models using computer-aided methods and PSG for the automatic classification of sleep stages [11], [12], [13].

These macrostructure-based sleep scoring rules, however, neglect temporary events like K-complexes and transient power fluctuations in frequency bands. As per the AASM recommendations, the definition of arousal only takes into account brief changes in brain activity. The characteristic of phasic events like delta bursts and K-complexes is identical to arousal; however, they are not regarded as arousal if the EEG shows no short-term increase in frequency [14], [15]. To compensate for the limitations of macrostructure-based sleep scoring, which often gives critical information on sleep quality and to characterize NREM sleep, a new sleep scoring technique based on microstructure has been introduced known as Cyclic Alternating Pattern (CAP) [16].

CAP can be defined as a physiological component of NREM sleep. It is the periodic EEG activity occurs over the course of NREM sleep. A CAP cycle consists of a pairof phases, commencing with a phase of activation in the EEG signals known as phase A (high-voltage slow-event), followed by periods of deactivation or background known as phase B (low-voltage fast-wave) which separate two successive phases A periods with an interval less than 60-sec [17]. At least two CAP cycles are needed to make up a CAP sequence. If the separation between two successive phases A is less than 2 sec then they are considered as a single phase A [18]. A CAP sequence always terminates at phase B. Non-CAP is defined as the absence of CAP for more than 60 seconds. phase A which ends a CAP sequence counts as non-CAP [19]. There is no upper limit to the quantity of CAP cycles or the span of a CAP sequence [20]. In healthy young people, the average time of a CAP sequence is approximately 150 seconds, with 6 CAP cycles [20]. A CAP sequence during

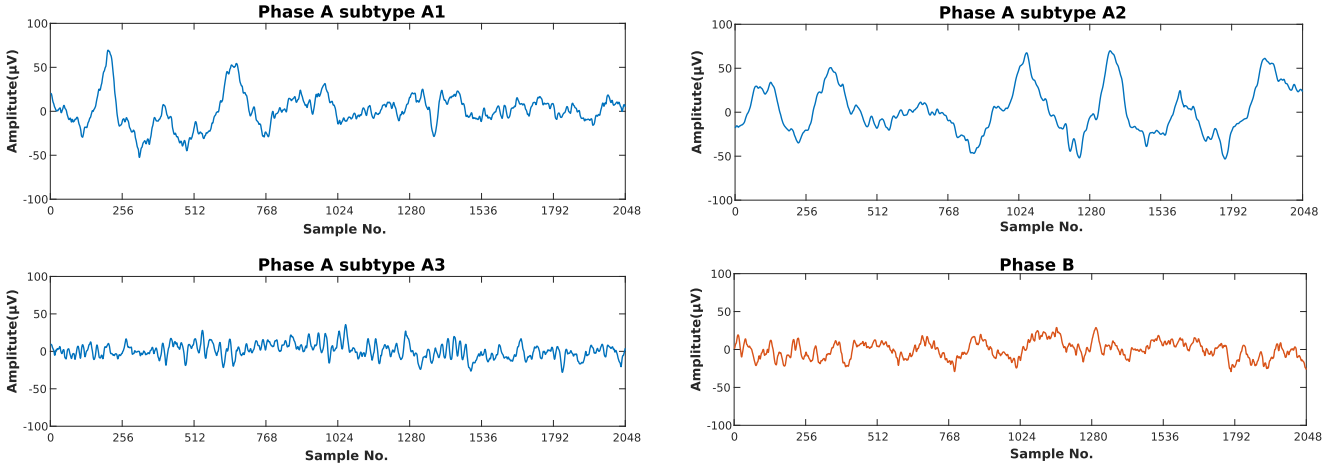

FIGURE 1. Typical waveform of phase A subtypes (A1, A2, and A3) and phase B obtained from healthy subject.

NREM sleep is not disrupted by a change in sleep stage if the CAP scoring requirements are satisfied. Because CAP sequences may span multiple successive sleep stages, they can involve a variety of phase A and phase B activities [16], [21]. CAP also appears as a well-defined indicator of brain activity occurring in situations of reduced alertness (sleep, coma), representing an instability in activities involving muscular, behavioral, and autonomic systems [19]. As the depth of sleep increases, the high amplitude and slow EEG waves increases, while low amplitude rapid rhythms become more prominent during REM sleep. Within phase A of CAP, there are three further sub-phases, namely A1, A2 and A3. The waveform of phase A subtypes (A1, A2, and A3) and phase B were obtained using healthy subject data from the CAPSD is shown in fig 1. The ratio of low-amplitude rapid rhythms (EEG desynchrony) to high-voltage slow waves (EEG synchrony) during phase A is used to classify phase A subtypes. Subtype A1 is distinguished by high amplitude slow waves that span more than 80% of the whole phase A length and low amplitude quick rhythms that cover 20% of the total phase A duration. Subtype A2 is distinguished by a combination of rapid and slow EEG waves. Low amplitude slow waves in phase A2 occupy about 20-50% of the whole length of phase A. Subtype A3 is characterized by dominating low amplitude rapid rhythms that occupy more than 50% of the phase A length. There are various CAP measures parameters like CAP rate, CAP time, and indices for phases A1, A2, and A3. The CAP rate can be defined as the ratio of CAP time to the total time of NREM sleep, expressed in percentage. The entire duration of all CAP sequences is called CAP time. It increases with the increase in CAP cycles. The number of phase A1 subtypes per hour of sleep is referred to as phase A1 index similarly phase A2 index and A3 index are defined [16]. CAP time rises as the number of CAP cycles increases. The CAP rate varies relatively little in healthy sleepers. It has been seen to change with age. The CAP rate does not vary significantly in individuals who sleep well, but it does vary with age. It is pretty low in babies (about 13%), progressively grows as the person ages, and reaches a relative high during the peripubertal period (approximately 62%), then there is a relative decrease for adults and middle age (around 37%), and a relative increase again in the elderly stage of life (55%). [19]. When sleep is interrupted by internal or external events, the CAP rate increases and its changes correspond with subjective judgments of sleep quality, with higher CAP rate values suggesting lower sleep quality [22]. As a result, detecting CAP phases and estimating CAP parameters is critical for proper sleep analysis. However, detecting CAP in humans is difficult and time-consuming procedure. Medical professionals manually examine and annotate CAP, leading to mistakes made by people and incorrect categorization. Hence, automated detection of CAP sleep phases is important.

Nowadays, numerous automated approaches have been suggested for the identifying of CAP phases. However, these research mainly focus on the classification of phase A vs non-phase A. There are very few studies done on A vs B phase classification and phase A subphases classification. The studies have done so far on A and B phase classification and phase A subtype classification have either used a huge number of differentiating features or obtained low classification performance. So, there is a need for new studies on A and B phase classification and phase A subtype classification. It is preferable for the model to use a limited number of features for training and testing, making it suitable for real-time applications, while still maintaining high accuracy in classification. In this proposed study, two classification task has been done first is phase A and phase B classification and the second is phase A subtypes classification. We have used PSG recordings of healthy as well as subjects suffering from five different disorders. The proposed model is developed using optimal biorthogonal filter and Hjorth parameters as features. We employed an XAI technique based on Shapley values to rank the extracted Hjorth features which provide insight into the classification ability. To the best of our

TABLE 1. The total number of samples from healthy individuals used in the CAP dataset, separated by subject.

	Healthy subjects						
Phase	n1	n2	n3	n5	n10	n11	Total
A1	1013	550	285	1307	703	796	4654
A2	354	327	284	157	159	270	1551
A3	548	597	494	377	445	386	2847
A-phase	1915	1474	1063	1841	1307	1452	9052
B-phase	4788	3041	2930	4221	1821	3187	19988
Total	6703	4515	3993	6062	3128	4639	29040

TABLE 2. The total number of samples in the CAP dataset, separated by specific sleep disorders.

	Sleep disorder types				
Type	Insomnia	Narcolepsy	NFLE	PLM	RBD
Subject	7	4	29	9	22
A1	3218	2088	25584	4832	11230
A2	1761	977	12743	3572	7350
A3	4800	2635	24666	8949	20620
A-phase	9779	5700	62993	17353	39200
B-phase	20686	11113	136540	34231	70201
Total	30465	16813	199533	51584	109401

knowledge, we are the first group to use XAI technique in the classification of sleep CAP phases. The created model outperformed current state-of-the-art techniques developed for the classification of CAP phases and sub-phases. The approach we developed is straightforward and requires minimal computational resources, making it suitable for use in clinical settings.

II. DATA ACQUISITION

The experimental dataset used in this study were taken from the CAP sleep database [23] (CAPSD) in the MIT-BIH database. The database is accessible to the public and contains sleep recordings of 108 individuals obtained from the Sleep Disorders Center of the Ospedale Maggiore of Parma, Italy. These recordings include 16 healthy individuals and 92 patients who have various sleep disorders from which 9 patients suffering from insomnia, 5 with narcolepsy, 40 with nocturnal frontal lobe epilepsy (NFLE), 10 with periodic leg movement (PLM), 22 with REM behavious disorder (RBD), and 4 with sleep-disordered breathing (SBD). The PSG recordings included at least three EEG channels, namely F3 or F4, C3 or C4, and A1 and A2, two EOG channels, two EMG channels, an ECG, and respiration signals along with some additional traces of bipolar EEG signals. The EEG recording with these channels was sampled at various sampling frequencies (100 Hz, 128 Hz, 200 Hz, and 512 Hz). Table 1 represents the number of samples collected from six healthy individuals, identified as n1, n2, n3, n5, n10, and n11. Table 2 represents the number of disordered subjects and samples in each phase that were included in the study who are affected by sleep disorders.

III. METHODOLOGY

The proposed method starts with the collecting PSG recordings from 77 subjects and extracting the electroencephalography (EEG) data from the recordings. The EEG data is then normalized and filtered to remove noise and other artifacts.

The labeled A&B phases and A1, A2, and A3 subphases are then segmented using windows of two seconds duration. Each EEG epoch of 2-sec duration or 1024 samples is then processed using an optimal frequency-localized orthogonal wavelet filter bank (OWFB), which breaks down each epoch into six separate frequency bands.

The labelled A&B phases and A1, A2, and A3 subphases are then segmented using two-second windows. An optimal frequency-localized OWFB is used to process each EEG epoch, which has a duration of 2 seconds or 1024 samples.

The Hjorth parameters were computed from decomposed subbands and used as discriminating features for the classification of the phases. After feature extraction, XAI - based feature ranking technique is applied to evaulate discriminating ability of extracted features [24]. A number of machine learning classifiers are employed to differentiate the features and choose the best classifier that performs well. To create a strong model and reduce the risk of overfitting, we use a ten-fold cross-validation approach during development.

A. DATA PREPROCESSING

Normal EEGs vary greatly and have a wide range of physiological differences [25]. Different characteristics, such as position, amplitude, frequency, shape, continuity, synchronization, symmetry, and reactivity of EEG waves, can be used to classify them [25]. However, frequency is the most often approach used for classifying EEG waveforms. The brain waves that are commonly referred to as delta have a frequency range of 0.5 to 4Hz, while theta waves range from 4 to 7Hz. Alpha waves fall within the range of 8 to 12Hz, sigma waves range from 12 to 16Hz, and beta waves range from 13 to 30Hz. These are the most widely studied waveforms [25]. As the relevant information lies in the range of frequency limited to the values under 35 Hz, EEG signals are filtered using a bandpass filter with an infinite impulse response (IIR), Butterworth filter of fourth order in order to eliminate noise artifacts and retain the relevant information [26], [27]. In accordance with AASM guidelines [9], the lower and upper cut-off frequencies for the filter are set to 0.5 Hz and 35 Hz respectively. After the filtering process, the signal is normalized so that the amplitude is reduced in a consistent manner over the range of 0 to 1.

The CAPSD contains annotations of phase A subtype as MCAP-A1, MCAP-A2, and MCAP-A3 along with their duration, provided by expert sleep scorers according to the rules outlined in Terzano's reference atlas [16]. The annotation of phase B is not directly provided in the database. We used the annotations to separate the CAP phase A

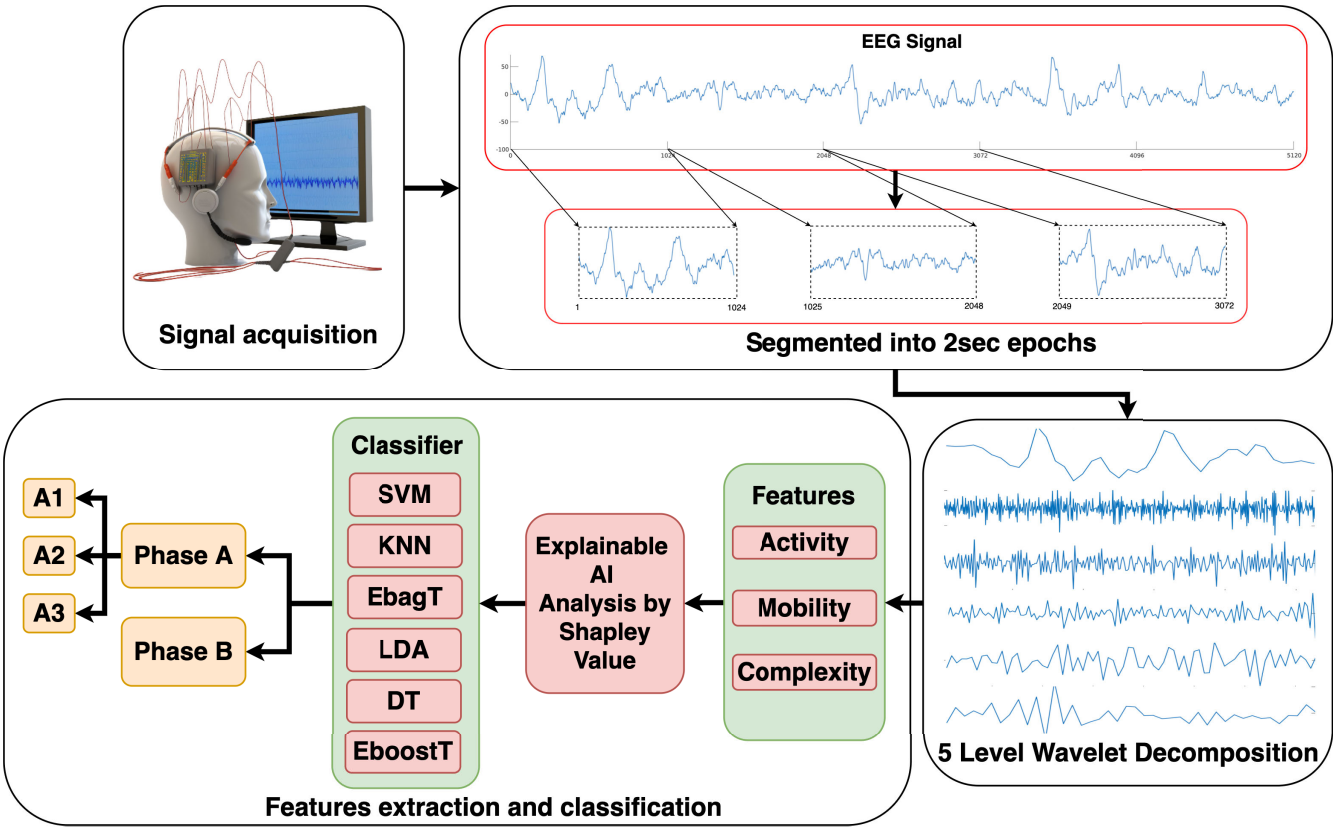

FIGURE 2. Flow diagram of the proposed study.

subtypes recording from the EEG signal during NREM sleep. After separation, each subtype signal is segmented into epochs of 2-sec duration each and labeled them as A1, A2, and A3. On combining the A1, A2, and A3 signals, a phase A signal is generated and we labeled it as "phase A". With the help of the duration of phase A provided in the CAP sleep database, we calculate phase B initiation and its duration. The phase A at which the CAP sequence is terminated is not considered in the CAP sequence, but it contains all of the characteristics of phase A. Thus, we utilized that phase A for the classification of phase A&B and the phase A subtype.

B. ORTHOGONAL FILTER BANK AND WAVELET DECOMPOSITION

EEG signals are often non-stationary, which means that their statistical properties change over time. This can make it challenging to analyze EEG signals using traditional techniques based on the Fourier transform, which assumes that the signal is stationary. In contrast, wavelet-based techniques are well-suited for analyzing non-stationary signals because they allow for the representation of a signal in both time and frequency domains and can capture local features in the signal that may vary over time [28], [29], [30]. There are many different wavelet filter banks that have been proposed and studied in the literature, covering a wide range of applications [28], [31], [32], [33], [34]. Among the various wavelet filter banks available, the OWFB has the ability to preserve the energy of the original signal during the decomposition process [35], [36], [37]. The OWFB with minimum frequency spread is used in the research study. It is a type of digital filter designed to have a specific frequency response. The frequency spread is a measure of the width of the filter's frequency response, and it is calculated by considering both the transition band and the pass/stopband of the filter [38]. The frequency spread design criterion is helpful because it takes into account the entire frequency spectrum of the filter rather than just the edge frequencies, which can be influenced by ripple amplitude specifications [39]. This makes the frequency spread a more comprehensive measure of the compactness of the filter, and it can be used to design filters with sharper roll-off and better performance. The equiripple filter method and the band-energy minimization method are other approaches that can be used to design filters with sharp roll-off, but they may not consider the entire frequency spectrum in the same way as the frequency-spread (bandwidth) approach [38], [39]. There are two ways to improve the bandwidth: using symbolic methods or solving a constrained optimization problem. This problem can be transformed into a convex optimization problem, specifically a semidefinite programming (SDP) problem, that enforces non-negativity constraints during optimization [40], [41], [42].

The importance of this technique is that it generates more precise and detailed data, encompassing all local and global minima [43], [44]. Wavelet decomposition is a technique used to decompose a signal into its frequency components. It involves the application of a wavelet transform to the signal, which decomposes the signal into a series of subbands or ''detail'' coefficients, each of which corresponds to a different frequency range. In this study, we used a five-level wavelet decomposition, which resulted in six sub-bands with frequency ranges of 0-1 Hz, 1-2 Hz, 2-4 Hz, 4-8 Hz, 8-16 Hz, and 16-32 Hz. The subband with the lowest frequency range, between 0 and 1 Hz, is designated as the approximation coefficient. The other subbands, which have higher frequencies, are referred to as detailed coefficients. The Figure 3 in the study illustrates the subbands resulting from the wavelet decomposition of epoches of A1, A2, and A3 subtype. These figures illustrate different frequency components of the signal for each subtype and may be used to identify patterns and trends in the data that may be indicative of certain conditions or events.

C. FEATURE EXTRACTION

In this study, we calculated 18 discriminating features for CAP phase A&B classification and phase A subtype classification, by computing Hjorth parameters (activity, mobility, and complexity) from each subband. The Hjorth parameters are a set of statistical features that can be used to characterize and extract features from time series data [45]. They are derived from the mean, variance, and autocovariance of the time series data. They are also widely used in EEG signal processing applications because they provide a robust and reliable way to characterize the dynamic properties of the signals. They are particularly useful for identifying patterns and trends in the data that may be indicative of certain conditions or events [45]. The Hjorth parameters are mathematically defined as follows:

The signal power is represented by the Hjorth activity parameter. It is the time-domain variance of a signal. It can be used to represent the frequency domain surface power spectrum. For any given time series x(t), activity is represented as the variance of signal x(t) and mathematically it can be expressed as in equation 1.

$$\text{Activity} = \text{Variance}(x(t)) \tag{1}$$

The Hjorth mobility is a metric of a signal's mean frequency. It is proportional to the standard deviation of the signal's power spectrum. Mobility is defined for any signal x(t) as the square root of the variance of the signal's first derivative divided by the variance of the signal x(t). It is given by equation 2.

$$\text{Mobility} = \sqrt{\frac{\text{Variance}(\frac{dx(t)}{dt})}{\text{Variance}(x(t))}} \tag{2}$$

The Hjorth complexity parameter is a measure of the difference in frequency. It measures how closely the shape of a signal resembles that of a pure sinusoidal signal. The parameter's value ranges between 0 and 1, with higher values indicating greater similarity to the reference signal. This metric provides a useful estimate of a signal's bandwidth. The complexity of a signal x(t) is defined as the ratio of the mobility of the first derivative of x(t) to the mobility of x(t), as shown in equation 3.

$$\text{Complexity} = \frac{\text{Mobility}(\frac{dx(t)}{dt})}{\text{Mobility}(x(t))} \tag{3}$$

D. MODEL CLASSIFICATION AND VALIDATION STRATEGY

Using single-channel EEG data, three Hjorth parameters are extracted from each of the six subbands to produce 18 time-domain features. After we finished extracting features from the data, multiple supervised machine-learning classifiers were employed to classify these features. These classifiers included K-nearest neighbor (KNN), support vector machines (SVM), ensemble bagged trees (EbagT), and ensemble boosted trees (EboostT). The model was developed by utilizing ten-fold cross-validation (CV) to evaluate the performance of machine learning models. This allows us to estimate the performance of the model on new data, and avoid overfitting issues. It is challenging to anticipate in advance which algorithm will perform optimally for a new dataset. We have utilized a trial-and-error approach to select the optimal algorithm among various classifiers. We selected the classifier which yielded the best classification performance and then fine-tuned its hyperparameters to further improve its performance. We implemented these algorithms and developed the model using the Statistics and Machine Learning Toolbox in MATLAB R2022b [46]. This toolbox provides a range of functions and tools for statistical analysis and machine learning tasks, such as importing and preprocessing data, fitting statistical models, making predictions, and evaluating model performance [46]. Through our simulations, we found that the ensemble bagged trees (EBT) and k-nearest neighbors (kNN) classifiers performed the best among all of the classifiers used.

IV. RESULTS

The performance of the developed model was evaluated using EEG recordings of 77 subjects acquired from the C4-A1 EEG channels for phase A&B (binary classification) and phase A subphases classification (three class classification). The database used to develop the model comprises recordings of healthy people and those with sleep disorders such as insomnia, NFLE, narcolepsy, SDB, PLM, and RBD. We used each subject's data independently to categorize the CAP. The database contains annotations for phase A and its belonging sleep stage. The phase A at which the CAP sequence is terminated is not considered in the CAP sequence, but it contains all of the characteristics of phase A. Thus, we utilized that phase A for the classification of phase A&B and the phase A subtype.

The entire experiment and training were carried out using MATLAB R2022b [46], which was installed on the

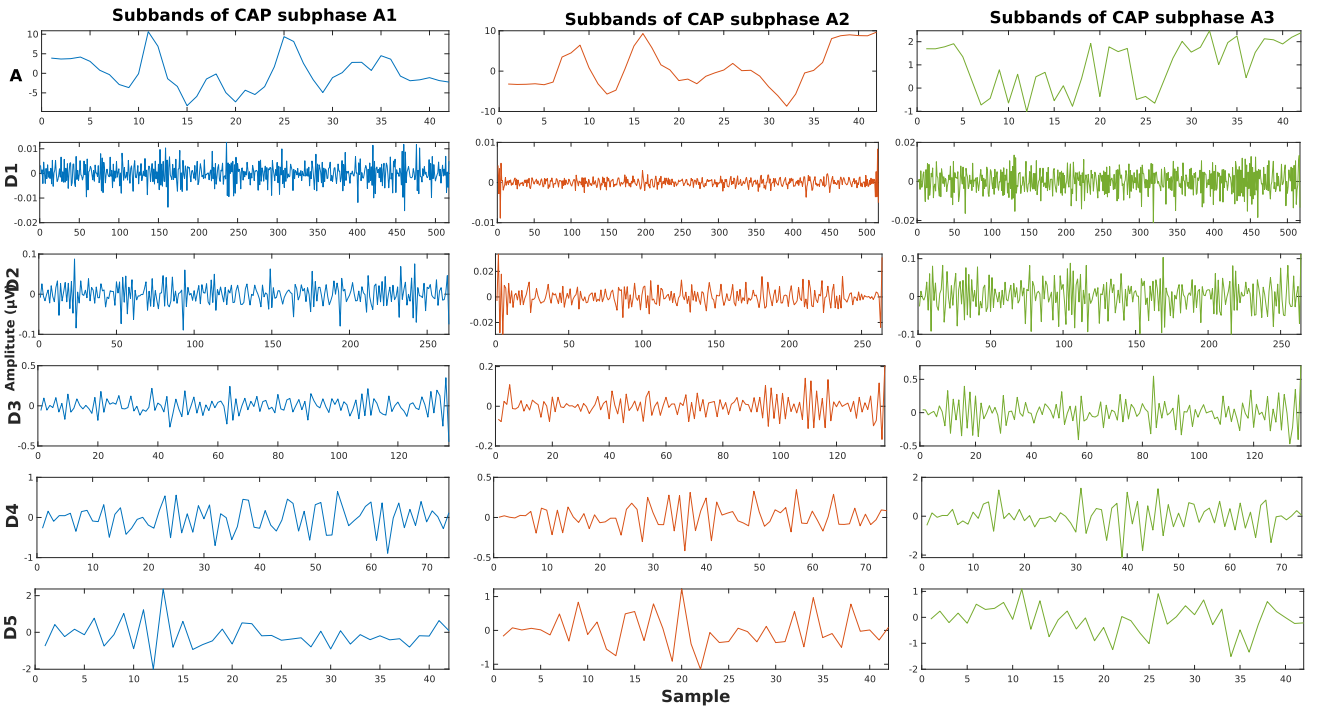

FIGURE 3. The waveform of subbands derived from the wavelet decomposition of CAP subphase A1, A2, and A3 for a 2-second epoch.

Windows 10 operating system. The system has a 2.10 GHz Intel(R) Xeon(R) Silver 4216 CPU and 32 GB of RAM. The performance of the classification was measured using various metrics such as average classification accuracy (ACA), precision (Pcn), recall (Rcl), F1-score (F1), Cohen's Kappa (κ) value, and area under the curve (AUC). It is challenging to predict which technique would perform optimally for our feature sets in advance, so we trained all classifiers using an iterative approach. After selecting the classifier with the best overall performance, we tweaked its hyperparameters to improved its performance even more. We determined that the KNN and EbagT algorithms had the greatest classification performance for the majority of classification tasks after a large number of simulations.

A. CAP PHASE A&B CLASSIFICATION PERFORMANCE

The EEG recording of 6 healthy subjects is used to extract 9052 epochs of A&B phase of two seconds durations each. Hjorth parameters were then computed for these epochs to create a feature set. This feature set was applied to numerous classifiers. For this classification task the EbagT classifier was found to have the best performance for classifying A and B phases The confusion matrix and performance parameters obtained for this classification task on healthy subjects are shown in Table 3. The maximum ACA obtained for A and B phase classification was 94.33%. In the tables AP denotes "A phase" and BP denotes "B Phase" of CAP.

TABLE 3. Performance parameters and confusion matrix obtained for Phase A&B classification in healthy subjects.

	Predictied class		Per-Class metrics		
True class	AP	BP	Pcn	Rcl	F1
AP	89.6%	10.4%	0.87	0.9	0.88
BP	6.1%	93.9%	0.95	0.94	0.95
Overall metrics		**ACA = 92.55%**		kappa =	0.828

TABLE 4. Performance parameters and confusion matrix obtained for Phase A&B classification in insomnia patients.

	Predictied class		Per-Class metrics		
True class	AP	BP	Pcn	Rcl	F1
AP	78.9%	21.1%	0.84	0.79	0.81
BP	7.0%	93.0%	0.9	0.93	0.92
Overall metrics		**ACA = 88.48%**		kappa =	0.731

The CAP sleep database consists of seven EEG recordings from patients with insomnia. These recordings have an average length of 575 minutes and were sampled at 512 Hz. A total of 30465 2-second epochs containing A&B phases were extracted from these recordings. The KNN classifier yielded the best ACA for the classification task. The maximum ACA for A&B phase classification of insomnia patients was 88.48%, as shown in Table 4.

TABLE 5. Performance parameters and confusion matrix obtained for Phase A&B classification in narcolepsy patients.

True class	Predicted class AP	BP	Per-Class metrics Pcn	Rcl	F1
AP	89.0%	11.0%	0.94	0.89	0.91
BP	2.9%	97.1%	0.95	0.97	0.96
Overall metrics		**ACA = 94.3%**	kappa =		0.872

TABLE 6. Performance parameters and confusion matrix obtained for Phase A&B classification in NFLE patients.

True class	Predicted class AP	BP	Per-class metrics Pcn	Rcl	F1
AP	75.4%	24.6%	0.8	0.75	0.78
BP	8.5%	91.5%	0.89	0.92	0.9
Overall metrics		**ACA = 86.4%**	kappa =		0.681

TABLE 7. Performance parameters and confusion matrix obtained for Phase A&B classification in PLM patients.

True class	Predicted class AP	BP	Per-class metrics Pcn	Rcl	F1
AP	79.8%	20.2%	0.86	0.8	0.83
BP	6.8%	93.2%	0.9	0.93	0.92
Overall metrics		**ACA = 88.7%**	kappa =		0.742

TABLE 8. Performance parameters and confusion matrix obtained for Phase A&B classification in RBD patients.

True class	Predicted class AP	BP	Per-class metrics Pcn	Rcl	F1
AP	74.8%	25.2%	0.81	0.75	0.78
BP	9.8%	90.2%	0.87	0.9	0.88
Overall metrics		**ACA = 84.6%**	kappa =		0.66

TABLE 9. Performance parameters and confusion matrix obtained for Phase A&B classification in combined 77 subjects.

True class	Predicted class AP	BP	Per-class metrics Pcn	Rcl	F1
AP	71.3%	28.7%	0.77	0.71	0.74
BP	10.3%	89.7%	0.86	0.9	0.88
Overall metrics		**ACA = 83.6%**	kappa =		0.62

TABLE 10. Performance parameters and confusion matrix obtained for Phase A subtype classification in healthy subjects.

True class	Predicted class A1	A2	A3	Per-class metrics Pcn	Rcl	F1
A1	94.5%	4.5%	1.1%	0.95	0.94	0.95
A2	12.8%	82.7%	4.4%	0.82	0.83	0.82
A3	1.7%	2.6%	95.7%	0.96	0.96	0.96
Overall metrics			**ACA = 92.85%**	kappa =		0.882

The CAP sleep database consists of EEG recordings from five individuals diagnosed with narcolepsy, each recording has a sampling rate of 512 Hz and an average length of 494 minutes. Four of these recordings were used to extract 16183 (2-second) epochs containing A&B phases. The KNN classifier was found to be the best for this classification task. The maximum ACA for A&B phase classification in narcolepsy patients was 94.3%, as shown in Table 5.

The EEG recording of 29 NFLE patients is used to extract 204533 epochs of A&B phase of two seconds duration. The average duration of these recordings is 505 min. The optimal performance was obtained using the EbagT classifier for the classification task considered in the study. The confusion matrix obtained along with the performance parameters corresponding to NFLE patients for classification is shown in Table 6. The maximum ACA obtained for A&B phase classification is 86.4%.

The CAP sleep database comprises nine EEG recordings from PLM patients, with an average duration of 431 minutes and a sampling frequency of 512 Hz. A total of 51584 (2-second) epochs containing A&B phases were extracted from these recordings. The KNN classifier provided the best ACA for the classification tasks. The maximum ACA for A&B phase classification in PLM patients was 88.7%, as shown in Table 7.

The CAP sleep database includes 22 EEG recordings from RBD patients, with an average duration of 514 minutes and a sampling frequency of 512 Hz. A total of 109401 (2-second) epochs containing A&B phases were extracted from these recordings. The KNN classifier provided the best ACA for the classification task. The maximum ACA for A&B phase classification in RBD patients was 84.6%, as shown in Table 8.

After individually analyzing the classification of phase A&B in sleep-disordered patients and healthy subjects, we combined the data from all 77 subjects and extracted a total of 436836 epochs of 2-sec duration corresponding to phase A&B. The EbagT classifier was found to be the most effective, in achieving a maximum ACA of 84.6%. This model accurately predicted 102696 out of 144077 Phase-A, and 262461 out of 292759 Phase-B, resulting pcn, recall values and AUC of 77.0%, 71.0%, and 90.0%, respectively. The performance parameters and confusion matrix for this classification task is shown in Table 9.

B. PHASE A SUBTYPE CLASSIFICATION PERFORMANCE

We analyzed the EEG recordings of 6 healthy subjects and extracted 29040 samples for the classification of Phase A subphases. After preprocessing the signals and extracting features, we found that the KNN classifier performed the best with a maximum ACA of 92.85%. The model was able to accurately predict 4396 out of 4654 A1 phases, 1283 out of 1551 A2 phases, and 2726 out of 2847 A3 phases, achieving high precision (95.0%) and recall values (94.0%). The performance parameters and confusion matrix for this classification task are shown in Table 10.

TABLE 11. Performance parameters and confusion matrix obtained for Phase A subtype classification in insomnia patients.

	Predictied			Per-class metrics		
True	A1	A2	A3	Pcn	Rcl	F1
A1	88.3%	6.2%	5.5%	0.9	0.88	0.89
A2	8.7%	79.8%	11.5%	0.8	0.8	0.8
A3	3.4%	3.0%	93.7%	0.92	0.94	0.93
Overall metrics			**ACA = 89.41%**		kappa =	8.82

TABLE 12. Performance parameters and confusion matrix obtained for Phase A subtype classification in narcolepsy patients.

	Predictied			Per-class metrics		
True	A1	A2	A3	Pcn	Rcl	F1
A1	94.5%	3.9%	1.6%	0.95	0.95	0.95
A2	8.4%	86.2%	5.4%	0.85	0.86	0.86
A3	1.2%	2.5%	96.3%	0.97	0.96	0.97
Overall metrics			**ACA = 93.9%**		kappa =	0.9

EEG recordings of 7 patients with insomnia disorder were analyzed to classify Phase A subphases. A total of 30465 samples were extracted from these recordings and preprocessed. The KNN classifier was determined to be the most effective, achieving an ACA of 89.41% for the classification of Phase A subtypes. The model showed high pcn (90.0%) and recall (94.0%), correctly predicting 2841 out of 3218 A1-phases, 1406 out of 1761 A2 phases, and 4496 out of 4800 A3 phases. The performance parameters and confusion matrix for this classification task are shown in Table 11.

For the classification of Phase A subphases in narcolepsy patients, we analyzed EEG recordings from 5 patients. A total of 16813 samples were extracted from these recordings and processed through signal preprocessing and feature extraction. After trying various classifiers, we found that the KNN classifier provided the best results with a maximum ACA of 93.9%. This model accurately predicted 1914 out of 2088 A1-phases, 842 out of 977 A2 phases, and 2537 out of 2635 A3-phases, resulting in high pcn (95.0%) and recall values (95.0%) highlighting the effectiveness of the classifier for narcolepsy. The results of this classification task, including performance parameters and confusion matrix, is shown in Table 12.

We analyzed EEG recordings from a total of 29 NFLE patients for the classification of Phase A subphases. A total of 199522 samples were extracted and processed through signal preprocessing and feature extraction. The KNN classifier was found to be the best option, achieving a maximum ACA of 80.92%. This model accurately predicted 21139 out of 25584 A1-phases, 8580 out of 12743 A2 phases, and 21254 out of 24666 A3-phases. Indicating relatively lower pcn (82.0%) and recall value (83.0%). The results of this classification task is shown in Table 13.

For the classification of Phase A subphases in PLM patients, we analyzed EEG recordings from 9 patients. A total of 51584 samples were extracted and processed through signal preprocessing and feature extraction. The KNN classifier was found to be the most effective, achieving a maximum ACA of 80.0%. This model accurately predicted 4204 out of 4832 A1-phases, 2849 out of 3572 A2 phases, and 8214 out of 8949 A3-phases, resulting in pcn and recall values of 88.0% and 87.0% respectively. The performance parameters and confusion matrix for this classification task can be seen in Table 14.

TABLE 13. Performance parameters and confusion matrix obtained for Phase A subtype classification in NFLE patients.

	Predictied			Per-class metrics		
True	A1	A2	A3	Pcn	Rcl	F1
A1	82.6%	10.4%	7.0%	0.82	0.83	0.82
A2	21.1%	67.3%	11.6%	0.67	0.67	0.67
A3	7.7%	6.1%	86.2%	0.87	0.86	0.86
Overall metrics			**ACA = 80.92%**		kappa =	0.702

TABLE 14. Performance parameters and confusion matrix obtained for Phase A subtype classification in PLM patients.

	Predictied			Per-class metrics		
True	A1	A2	A3	Pcn	Rcl	F1
A1	87.0%	6.9%	6.1%	0.88	0.87	0.88
A2	8.5%	79.8%	11.7%	0.78	0.8	0.79
A3	3.0%	5.2%	91.8%	0.92	0.92	0.92
Overall metrics			**ACA = 88.0%**		kappa =	0.804

TABLE 15. Performance parameters and confusion matrix obtained for Phase A subtype classification in RBD patients.

	Predictied			Per-class metrics		
True	A1	A2	A3	Pcn	Rcl	F1
A1	83.6%	7.9%	8.5%	0.82	0.84	0.83
A2	13.4%	73.4%	13.2%	0.74	0.73	0.74
A3	5.5%	4.8%	89.7%	0.91	0.9	0.9
Overall metrics			**ACA = 84.9%**		kappa =	0.751

For the classification of Phase A subphases in RBD patients, we analyzed EEG recordings from a total of 22 patients. A total of 109401 samples were extracted and processed through signal preprocessing and feature extraction. The KNN classifier was found to be the most effective, achieving a maximum ACA of 84.9%. This model accurately predicted 9383 out of 11230 A1-phases, 5397 out of 7350 A2 phases, and 18488 out of 20620 A3-phases, resulting in pcn and recall values of 82.0% and 84.0% respectively. The performance parameters and confusion matrix for this classification task is shown in Table 15.

After individually analyzing the classification of phase A subphases in sleep disordered patients and healthy subjects, we combined the data from all 77 subjects and extracted a total of 144077 epochs of 2-sec duration corresponding to phase A subphases. The KNN classifier was found to be the most effective, achieving a maximum ACA of 78.8%. This

TABLE 16. Performance parameters and confusion matrix obtained for Phase A subtype classification in combined 77 subjects.

	Predictied			Per-class metrics		
True	A1	A2	A3	Pcn	Rcl	F1
A1	79.9%	10.8%	9.2%	0.79	0.8	0.8
A2	20.4%	63.1%	16.4%	0.63	0.63	0.63
A3	8.0%	7.4%	84.6%	0.85	0.85	0.85
Overall metrics			ACA = 78.8%		kappa =	0.665

model accurately predicted 41255 out of 51606 A1-phases, 17651 out of 27954 A2 phases, and 54604 out of 64517 A3-phases, resulting in pcn, recall values and AUC of 79.0%, 80.0%, and 84.0% respectively. The performance parameters and confusion matrix for this classification task is shown in Table 16.

C. EXPLAINABLE AI (XAI) USING SHAPLEY ANALYSIS

Feature ranking is important because it helps to identify the most relevant features for a given classification task. [47] By ranking features in order of importance, it can help to reduce the dimensionality of the data, which can make it easier to visualize and analyze. Additionally, feature ranking can help to improve the performance of machine learning models by identifying the most informative features and discarding those that are less relevant [47]. One of the most prominent method for feature ranking in machine learning is SHAP (SHapley Additive exPlanations) method [48]. It is a method that uses the concept of Shapley values to provide feature importance scores for any machine learning model. This method for feature ranking assigns a score to each feature based on its contribution to the overall prediction made by a machine learning model [24], [49]. The method takes into account the interactions between features and assigns a score based on the marginal contribution of each feature to the overall prediction. It assigns a score to each feature, indicating how much the model's accuracy would decrease if that feature were removed [49]. Features with high Shapely values have a greater impact on the model's predictions, and removing them would cause a greater decrease in accuracy. This method can be used to identify the most important features for a given problem and also to understand how different features are contributing to the final prediction [49]. It is an effective method for feature selection and feature importance ranking [50].

In this study, we calculated the Shapley value for two cases. In the first case, we used the 18 features of phase A and B from healthy subjects and ranked its features using the Shapley value, as shown in Figure 4a. In the second case, we used the 18 features of phase A subtype from healthy subjects and ranked its features using the Shapley value, as shown in Figure 4b. The Shapley beeswarm plot shown in Figure 4 depicts that the features at the top of the plot have a greater impact on the model's prediction than those at the bottom. In the Shapley beeswarm plot, the red dots denote features that contribute more to the model's prediction, and blue dots denote features that contribute less to the model's prediction. From our analysis, we found that in the first case, for phase A and B classification, features from 'Activity (D1)' to 'Activity (D4)' have more red dots compared to blue or purple dots, indicating that they have a greater significance in affecting the model's output as compared to other features. In the second case, for phase A subtype classification, features from 'Activity (D1)' to 'Activity (D4)' have more red dots compared to blue or purple dots, indicating they have a greater significance in affecting the model's output than other features. This implies that in both cases, features 'Activity (D1)' to 'Activity (D4)' which were obtained through a combination of wavelet decomposition and Hjorth parameter have been found to be highly effective for classification. These features may be employed in a machine learning model to identify CAP phase A and B, and phase A subphases.

V. DISCUSSION

There are few works available on the automated classification of the microstructure of CAP (Phase A&B and phase A subphases). On the other side, there are several research available, based on the automated classification of sleep macrostructures events, such as sleep stage scoring and identification of sleep disorders. There are limited number of studies available on identifying the phases of CAP that have included individuals with sleep disorders, with the few exceptions of Mendonca et al. [56], Hartmann et al. [57], Sharma et al. [51], and Murarka et al. [7] who included both healthy individuals and patients with sleep disorders. From studies that classify the microstructure of CAP the majority classified phase A because CAPSD (CAP sleep database) only contains annotation of phase A subtypes, the annotations for B phase is not available in the CAPSD. Sharma et al. [55] and Dhok et al. [52] classified the A&B phases of the CAP using healthy subjects. Sharma et al. [55] achieved their highest performance using 12 features, while Dhok et al. [52] achieved their highest performance using 121 features. Mendez et al. [58] in their study used an unbalanced data set, comprising 3963 occurrences of Phase A subtypes from 10 healthy individuals. They applied a KNN classifier with different features such as sample entropy, energy, Tsallis entropy, frequency band indices, and standard deviation. They reported an accuracy score (ACA) of 80%, sensitivity of 80%, and specificity of 70%. Dhok et al. [52] used balanced data set of six healthy participants from the CAP sleep database, with 4653 samples of phase A & phase B each, for automatic CAP phase classification. They achieved 72.35% ACA using Wigner-Ville distribution-based feature extraction and a support vector machine (SVM) classifier. Mendonca et al. [56] developed a classification technique that uses time series analysis and a matrix of lags, coupled with an SVM classifier. The developed method achieved an ACA of 77% for indirect estimation of the CAP cycles using ECG signals with a duration of 60 seconds. Loh et al. [54] classified the A&B phases of the CAP using a 1D convolutional

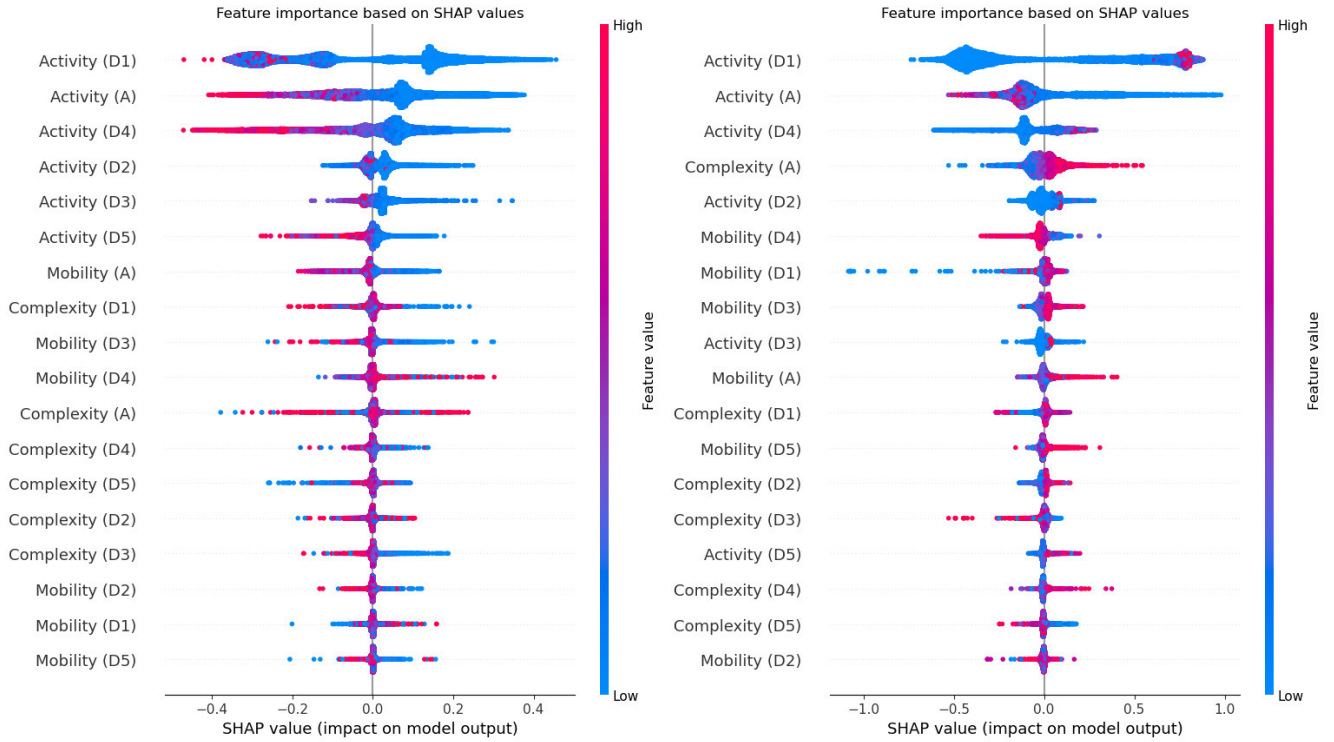

(a) Phase A & B (b) Phase A subtypes

FIGURE 4. Results of shapley features performed on KNN classifier.

TABLE 17. Comparison of our work on the automated phase A&B classification with the previous works conducted using the same database.

Sleep disorder type	Study	Performance measures (%)					Classifier
		ACA	Precision	Sensitivity	Specificity	F1 Score	
Insomnia	Sharma M et al. [51]	71.4	73	67.2	75.7	70	EBagT
	Murarka et al. [7]	70.88	81.82	56.52	86.41	66.86	1D-CNN
	Our work	**88.48**	**84.24**	**78.87**	**93.02**	**81.47**	KNN
NFLE	Sharma M et al. [51]	77.4	79	75	79.60	77	SVM
	Murarka et al. [7]	76.68	74.08	81.24	72.23	77.49	1D-CNN
	Our work	**86.43**	**80.38**	**75.43**	**91.50**	**77.83**	E-bagT
Narcolepsy	Sharma M et al. [51]	71.8	73	70	73.90	71	EBoosT
	Murarka et al. [7]	82.21	82.09	82.60	82.34	81.82	1D-CNN
	Our work	**94.33**	**93.95**	**89.02**	**97.06**	**91.42**	KNN
RBD	Sharma M et al. [51]	66	68	60	71.8	64	EBagT
	Murarka et al. [7]	79.48	**84.92**	72.30	86.84	**78.10**	1D-CNN
	Our work	**84.67**	80.93	**74.84**	**90.15**	77.77	KNN
PLM	Sharma M et al. [51]	71.9	74	70	75.8	71	EBoosT
	Murarka et al. [7]	78.72	83.98	71.64	85.99	77.32	1D-CNN
	Our work	**88.68**	**85.60**	**79.77**	**93.20**	**82.58**	KNN

neural network (CNN) and achieved an ACA of 73.64%, but their study was also limited to healthy participants. However, their model required a higher level of processing power due to the more number of trainable parameters. Mariani et al. [59] discovered that Hjorth activity was a more effective descriptor for CAP A phases, resulting in improved performance in classifying between Phase A and Phase B, which supports the results of our study. Table 18 summarises several CAP detection studies that employed EEG data from the CAPSD.

The work done by Sharma et al. [51] focused on classifying Phase A and Phase B of CAP, whereas this work aimed to provide a comprehensive classification by including subtypes of A-Phase, namely A1, A2, and A3. This approach aims to provide a more detailed evaluation of cyclic changes during sleep, which is crucial in clinical settings. Also, we attempted

TABLE 18. Comparison of our work on phase A and phase B classification with other studies using the same database.

Study	Method	Number of subjects	Performance measures (%)			
			ACA	Sensitivity	Specificity	F1-Score
Dhok et al. [52]	Renyi Entropy based on Wigner-Ville and SVM	6 (healthy)	87.45	87.75	52.09	73
Mendonca et al. [53]	Time series analysis based on SVM	9(Healthy), 4 (SBD), 1 (bruxism)	79	76	80	-
Machado et al. [54]	Mutiple features with KNN, SVM and DA classifier	30 (NFLE)	76	77	79	-
Sharma et al. [55]	optimal biorthogonal wavelet filter based Tsallis, approximate Entropy fetures	6 (healthy)	87.50	51.89	87.53	-
Sharma et al. [51]	Optimal wavelet based Hjorth and entropy features	77 (Healthy and disordered included)	75.7	75.7	74	77.3
Murarka et al. [7]	1-D CNN	75 (Healthy and disordered included)	78.84	73.44	84.26	77.68
Our work	Hjorth parametre features based on Optimal wavelet filter	77 (Healthy and disordered included)	**92.55**	**89.57**	**93.9**	**88.23**

to fill the research gap identified by Sharma et al. [51], who suggested that machine learning models should be developed to classify the subtypes of Phase A. Sharma et al. [51] used a combination of Hjorth parameters and wavelet entropy to extract 48 features for classification, whereas we use only 18 Hjorth parameters. Hence, we reduced the computational complexity of the system compared to the previous work by Sharma et al. [51]. Furthermore, while their model used two EEG channels, we use a single EEG channel (C4-A1), which simplified the model. Our results showed that the KNN classification algorithm was the most effective in our model, as opposed to the top-performing Ensemble of the boosted tree (Eboost) and the Ensemble of the bagged tree (EbagT) used by Sharma et al. [51]. The advantages of KNN include its simplicity and shorter training time, making it well-suited for practical applications in real-life scenarios. A comparison between our method and Sharma et al. [51] can be found in Table 17. Sharma et al. [51] considered the classification task of A phases with respect to non-A phases in their work. They labeled all non-A phases occurring during the NREM sleep stage as B phases. However, it should be noted that according to AASM guidelines, not all non-A phases are necessarily B phases (B phases are a subset of non-A phases). In this work, we followed the guidelines of the AASM for precise segregation of non-A and B phases. This accurate and rigorous approach to labeling A and B phases has led to a significant improvement in accuracy. Furthermore, it may be noted that the number of A and B phases considered for the classification task in Sharma et al. [51]'s work is equal by not considering all epochs of A-phases. However, in our work, we have considered all epochs, and therefore the numbers of A and B phases are not the same, as shown in Table 1 and Table 2.

Recently, Murarka et al. [7] classified CAP phases for both healthy and disordered individuals using 1-D CNN without extracting the features. Table 17 presented a comparison of our work with state of art techniques on the classification of phase A&B with the C4-A1 channels for narcolepsy, RBD, PLM, NFLE, and insomnia patients. Murarka et al.'s [7] model for insomnia achieved an ACA of 70.88%, while our model had an ACA of 88.48%, an improvement of 17.6%. Murarka et al.'s [7] model had precision of 81.82%, sensitivity of 56.52%, specificity of 86.41%, and F1 score of 66.86%. Our model obtained a precision of 84.24%, sensitivity of 78.87%, specificity of 93.02%, and F1 score of 81.47%. Our model for insomnia showed improvements in each of these performance parameters, making it an effective classifier for insomnia. Murarka et al.'s [7] model for NFLE had an ACA of 76.68%, a precision of 74.08%, sensitivity of 81.24%, specificity of 72.23%, and F1 score of 77.49%. Our model was able to improve these results, achieving an ACA of 86.43%, with an improvement of 9.75%. Our model also had a precision of 80.38%, sensitivity of 75.43%, specificity of 91.50%, and F1 score of 77.83%. For narcolepsy, our model outperformed Murarka et al.'s [7] model in all performance measures. With an ACA of 94.33%, precision of 93.95%, sensitivity of 89.02%, specificity of 97.06%, and F1 score of 91.42%, our model was approximately 10% better in each performance measure. Our model also showed a slight improvement over Murarka et al.'s [7] model for RBD, with an ACA of 84.67% compared to 79.48%. The other performance measures, including precision, sensitivity, specificity, and F1 score, were similar between the two models. Our model for PLM had an ACA of 88.68%, a significant improvement of 15.96% over Murarka et al.'s [7] model, which had an ACA of 78.72%. Our model also outperformed theirs for precision (85.60% vs 83.98%), sensitivity (79.77% vs 71.64), specificity (93.20% vs 85.99), and F1 score (82.58% vs 77.32%). Our model for PLM showed significant improvements in each of these performance parameters, making it a highly

TABLE 19. Comparision of our work on phase A subtype classification with other studies using the same database.

Disorder type	Study	Method	ACA (%)	Classifier
Healthy	Mendonça et al. [60]	Heuristic oriented search algorithm based on 1-D CNN	82	1D-CNN
	Our work		**92.85**	KNN
Healthy	Mendez et al. [61]	Multiple features with KNN classifier	82.23	KNN
	Our work		**92.85**	KNN
Healthy	Hartmann et al. [57]	Multiple features with variable LSTM network	81.89	LSTM
	Our work		**92.85**	KNN
NFLE	Machado et al. [62]	Mutiple features with KNN , SVM and DA classifier	61	SVM, KNN
	Our work		**80.92**	KNN

effective model. Overall, the results show that our model outperformed Murarka et al.'s [7] model in terms of ACA, precision, sensitivity, specificity, and F1 score for all sleep disorders (insomnia, narcolepsy, RBD, and PLM). These improvements justifies the superiority of our model over the state-of-the-art techniques for all sleep disorders.

It can be noted from Tables 17 and 18 that, there are few works available on classifying CAP phase A subtypes. Further research in this area may be necessary to better understand and classify CAP phase A subtypes. Table 19 shows the comparision of our work on phase A subtype classification with other studies. In this study, we have classified CAP phase A subtypes separately for each disordered type, and also combined them for a more comprehensive analysis. Mendonca et al. [60] developed a metric called the A phase index (API) using deep learning and a 1D-CNN classifier for classification. Their method was able to classify A subtypes with an ACA of 82% using 27 subjects. Hartmann et al. [57] used data from the CAPSD to examine 16 healthy sleepers and 30 NFLE patients. The duration of the EEG epochs analyzed in this study ranged from 1-3 seconds. They reported an ACA of 81.89% in the classification of phase A subtypes using a group of healthy participants. Their model obtained an ACA of 78.27% on a group of NFLE subjects. Our proposed model for classifying phase A subtypes used several different groups of subjects. When applied to healthy subjects, the model achieved an ACA of 92.85%. It achieved an ACA of 89.41%, 93.9%, 80.9% 88.0%, and 84.9% for individuals with insomnia, narcolepsy,NFLE, PLM, and RBD, respectively. Our proposed model obtained an overall ACA was 78.8% when considered sleep disorders and healthy subjects combined which is shown in table 16. Our proposed model yielded superior results compared to a majority of previous studies.

Some of the advantages of our study are given below:

- We utilized an openly accessible CAP sleep database to facilitate reproducibility and made it possible for other researchers to evaluate their own research in relation to this study.
- We expanded our sample size by incorporating participants from six distinct categories of the CAP database comprising individuals with insomnia, PLM, NFLE, RBD, narcolepsy, in addition to healthy subjects.
- To the best of our knowledge this is the only study that incorporates 6 classes and provide performance metrics for each class.
- Used a single EEG channel to improve patient comfort, and this approach ultimately resulted in better performance.
- We employed an XAI technique based on Shapley values to rank the extracted Hjorth features which provide insight into the classification ability. To the best of our knowledge, we are the first group to use XAI technique in the classification of sleep CAP phases.
- In contrast to other studies, the proposed method uses fewer features, leading to a reduction in computational complexity.
- Our developed model is simple and does not involve much computational complexity, making it suitable for deployment in real-time applications by medical practitioners.

There is a need for further research using heart rate variability (HRV) and electrocardiography (ECG) signals, acquired from photoplethysmography (PPG) signals, for the identification of CAP phases and subphases.

PPG signals, which use light to measure HRV, are particularly well-suited for use in wearable devices for CAP phases and subphases detection. The use of these signals in wearable devices has the potential to make CAP detection more accessible and convenient. PPG signals, which use light to measure HRV, are particularly well-suited for use in wearable devices designed for detecting CAP phases and subphases. The use of these signals in wearable devices has the potential to make CAP detection more accessible and convenient.

VI. CONCLUSION

In this study, we developed a novel algorithm for detecting the different phases of CAP using EEG signals. KNN and EbagT classifiers are used to distinguish A&B phases of CAP and also to identify the A1, A2, and A3 subphases within the A phase, utilizing single-channel EEG signals. We evaluated the algorithms on subjects, both healthy and those with one of five sleep disorders. We used a combination of wavelet-bases techniques and machine learning methods to develop the algorithms, and the results showed that they were able to achieve promising performance in detecting

the different CAP phases. We used an optimal filter bank with minimized orthogonal properties and mean squared bandwidth during the signal preprocessing stage to perform decomposition. We used Hjorth parameters as features, and employed optimally tuned KNN and EbagT classifiers, which yielded promising performance. We employed XAI-based feature ranking method to provide insights into the model's decision-making process, and aid clinicians to trust our model. The results showed that the algorithms were able to achieve promising performance in detecting the different CAP phases, with average classification accuracy of 91.6% for healthy subjects and 94.33%, 88.68%, 86.3%, 88.5%, and 84.43% for narcolepsy, PLM, RBD, insomnia, and NFLE subjects, respectively, when categorizing phases A&B. The maximum ACA was obtained for narcolepsy patients, at 94.33% for phase A&B classification. When categorizing A subphases (A1, A2, A3), the model was able achieved an average classification accuracy of 92.85% for healthy subjects and 93.9%, 88.0%, 84.9%, 89.41%, and 80.92% for narcolepsy, PLM, RBD, insomnia, and NFLE subjects, respectively. Before implementing the proposed model in a clinical setting, it is necessary to test it using a diverse and large dataset. Our developed system is easy to use, automated, and designed with XAI technique, which can potentially alleviate the difficulties encountered by sleep specialists during scoring of CAP phases. Our future goal is to create a model based on HRV signals that are derived from PPG signals to identify of CAP phases and subphases which will reduce the bandwidth and computational time of the system.

REFERENCES

[1] J. W. Cho and J. F. Duffy, "Sleep, sleep disorders, and sexual dysfunction," *World J. Men's Health*, vol. 37, no. 3, pp. 261–275, 2019.

[2] M. Walker, *Why we Sleep: Unlocking the Power of Sleep and Dreams*. New York, NY, USA: Simon and Schuster, 2017.

[3] D. J. Buysse, C. F. Reynolds, T. H. Monk, S. R. Berman, and D. J. Kupfer, "The Pittsburgh sleep quality index: A new instrument for psychiatric practice and research," *Psychiatry Res.*, vol. 28, no. 2, pp. 193–213, May 1989.

[4] *Polysomnography (Sleep Study)*, Mayo Clinic, Rochester, MN, USA, Dec. 2020.

[5] *What is Polysomnography*, Healthline Media, San Francisco, CA, USA, Dec. 2022.

[6] M. Sharma, S. Singh, A. Kumar, R. S. Tan, and U. R. Acharya, "Automated detection of shockable and non-shockable arrhythmia using novel wavelet-based ECG features," *Comput. Biol. Med.*, vol. 115, Dec. 2019, Art. no. 103446.

[7] S. Murarka, A. Wadichar, A. Bhurane, M. Sharma, and U. R. Acharya, "Automated classification of cyclic alternating pattern sleep phases in healthy and sleep-disordered subjects using convolutional neural network," *Comput. Biol. Med.*, vol. 146, Jul. 2022, Art. no. 105594.

[8] T. Hori, Y. Sugita, E. Koga, S. Shirakawa, K. Inoue, S. Uchida, H. Kuwahara, M. Kousaka, T. Kobayashi, Y. Tsuji, M. Terashima, K. Fukuda, and N. Fukuda, "Proposed supplements and amendments to 'a manual of standardized terminology, techniques and scoring system for sleep stages of human subjects', the rechtschaffen & Kales (1968) standard," *Psychiatry Clin. Neurosci.*, vol. 55, no. 3, pp. 305–310, Jun. 2001.

[9] C. Iber, "The AASM manual for the scoring of sleep and associated events," *Terminol. Tech. Specification*, 2007.

[10] M. Sharma, J. Tiwari, V. Patel, and U. R. Acharya, "Automated identification of sleep disorder types using triplet half-band filter and ensemble machine learning techniques with EEG signals," *Electronics*, vol. 10, no. 13, p. 1531, Jun. 2021.

[11] O. Faust, H. Razaghi, R. Barika, E. J. Ciaccio, and U. R. Acharya, "A review of automated sleep stage scoring based on physiological signals for the new millennia," *Comput. Methods Programs Biomed.*, vol. 176, pp. 81–91, Jul. 2019.

[12] U. R. Acharya, S. Bhat, O. Faust, H. Adeli, E. C.-P. Chua, W. J. E. Lim, and J. E. W. Koh, "Nonlinear dynamics measures for automated EEG-based sleep stage detection," *Eur. Neurol.*, vol. 74, nos. 5–6, pp. 268–287, 2015.

[13] H. W. Loh, C. P. Ooi, J. Vicnesh, S. L. Oh, O. Faust, A. Gertych, and U. R. Acharya, "Automated detection of sleep stages using deep learning techniques: A systematic review of the last decade (2010–2020)," *Appl. Sci.*, vol. 10, no. 24, p. 8963, Dec. 2020.

[14] M. G. Terzano and L. Parrino, "Origin and significance of the cyclic alternating pattern (CAP)," *Sleep Med. Rev.*, vol. 4, no. 1, pp. 101–123, Feb. 2000.

[15] S. Hartmann, O. Bruni, R. Ferri, S. Redline, and M. Baumert, "Characterization of cyclic alternating pattern during sleep in older men and women using large population studies," *Sleep*, vol. 43, no. 7, Jul. 2020, Art. no. zsaa016.

[16] M. G. Terzano, L. Parrino, A. Smerieri, R. Chervin, S. Chokroverty, C. Guilleminault, M. Hirshkowitz, M. Mahowald, H. Moldofsky, A. Rosa, R. Thomas, and A. Walters, "Atlas, rules, and recording techniques for the scoring of cyclic alternating pattern (CAP) in human sleep," *Sleep Med.*, vol. 3, no. 2, pp. 187–199, Mar. 2002.

[17] L. Parrino, M. Boselli, M. C. Spaggiari, A. Smerieri, and M. G. Terzano, "Cyclic alternating pattern (CAP) in normal sleep: Polysomnographic parameters in different age groups," *Electroencephalogr. Clin. Neurophysiol.*, vol. 107, no. 6, pp. 439–450, Dec. 1998.

[18] R. Ferri, O. Bruni, S. Miano, G. Plazzi, K. Spruyt, D. Gozal, and M. G. Terzano, "The time structure of the cyclic alternating pattern during sleep," *Sleep*, vol. 29, no. 5, pp. 693–699, May 2006.

[19] L. Parrino, R. Ferri, O. Bruni, and M. G. Terzano, "Cyclic alternating pattern (CAP): The marker of sleep instability," *Sleep Med. Rev.*, vol. 16, no. 1, pp. 27–45, Feb. 2012.

[20] A. Smerieri, L. Parrino, M. Agosti, R. Ferri, and M. G. Terzano, "Cyclic alternating pattern sequences and non-cyclic alternating pattern periods in human sleep," *Clin. Neurophysiol.*, vol. 118, no. 10, pp. 2305–2313, Oct. 2007.

[21] M. Terzano, "Mutural cooperation between cyclic alternating pattern and major dynamic events of sleep," *Insomnia Imidazopyridines*, pp. 262–270, 1990.

[22] M. Terzano, L. Parrino, G. Fioriti, M. Spaggiari, and A. Piroli, "Morphologic and functional features of cyclic alternating pattern (CAP) sequences in normal NREM sleep," *Funct. Neurol.*, vol. 1, no. 1, pp. 29–41, 1986.

[23] A. L. Goldberger, L. A. N. Amaral, L. Glass, J. M. Hausdorff, P. C. Ivanov, R. G. Mark, J. E. Mietus, G. B. Moody, C.-K. Peng, and H. E. Stanley, "PhysioBank, PhysioToolkit, and PhysioNet: Components of a new research resource for complex physiologic signals," *Circulation*, vol. 101, no. 23, pp. 215–220, Jun. 2000.

[24] H. W. Loh, C. P. Ooi, S. Seoni, P. D. Barua, F. Molinari, and U. R. Acharya, "Application of explainable artificial intelligence for healthcare: A systematic review of the last decade (2011–2022)," *Comput. Methods Programs Biomed.*, vol. 226, Nov. 2022, Art. no. 107161.

[25] C. S. Nayak and A. C. Anilkumar. (Jul. 25, 2022). *Eeg Normal Waveforms—StatPearls—NCBI Bookshelf*. Accessed: Dec. 22, 2022. [Online]. Available: https://www.ncbi.nlm.nih.gov/books/NBK539805/

[26] X. Jiang, G.-B. Bian, and Z. Tian, "Removal of artifacts from EEG signals: A review," *Sensors*, vol. 19, no. 5, p. 987, Feb. 2019.

[27] C. Q. Lai, H. Ibrahim, M. Z. Abdullah, J. M. Abdullah, S. A. Suandi, and A. Azman, "Artifacts and noise removal for electroencephalogram (EEG): A literature review," in *Proc. IEEE Symp. Comput. Appl. Ind. Electron. (ISCAIE)*, Apr. 2018, pp. 326–332.

[28] M. Sharma and U. R. Acharya, "Automated detection of schizophrenia using optimal wavelet-based ℓ_1 norm features extracted from single-channel EEG," *Cognit. Neurodynamics*, vol. 15, no. 4, pp. 661–674, 2021.

[29] J. S. Rajput, M. Sharma, R. S. Tan, and U. R. Acharya, "Automated detection of severity of hypertension ECG signals using an optimal bi-orthogonal wavelet filter bank," *Comput. Biol. Med.*, vol. 123, Aug. 2020, Art. no. 103924.

[30] M. Sharma, S. Patel, and U. R. Acharya, "Automated detection of abnormal EEG signals using localized wavelet filter banks," *Pattern Recognit. Lett.*, vol. 133, pp. 188–194, May 2020.

[31] D. Bhati, M. Sharma, R. B. Pachori, S. S. Nair, and V. M. Gadre, "Design of time-frequency optimal three-band wavelet filter banks with unit Sobolev regularity using frequency domain sampling," *Circuits, Syst., Signal Process.*, vol. 35, no. 12, pp. 4501–4531, Dec. 2016.

[32] M. Sharma, A. Dhere, R. B. Pachori, and U. R. Acharya, "An automatic detection of focal EEG signals using new class of time-frequency localized orthogonal wavelet filter banks," *Knowl.-Based Syst.*, vol. 118, pp. 217–227, Feb. 2017.
[33] M. Sharma, A. Dhere, R. B. Pachori, and V. M. Gadre, "Optimal duration-bandwidth localized antisymmetric biorthogonal wavelet filters," *Signal Process.*, vol. 134, pp. 87–99, May 2017.
[34] M. Sharma, R.-S. Tan, and U. R. Acharya, "Detection of shockable ventricular arrhythmia using optimal orthogonal wavelet filters," *Neural Comput. Appl.*, vol. 32, no. 20, pp. 15869–15884, Oct. 2020.
[35] M. Sharma, D. Deb, and U. R. Acharya, "A novel three-band orthogonal wavelet filter bank method for an automated identification of alcoholic EEG signals," *Int. J. Speech Technol.*, pp. 1368–1378, Aug. 2017.
[36] M. Sharma and U. R. Acharya, "Analysis of knee-joint vibroarthographic signals using bandwidth-duration localized three-channel filter bank," *Comput. Electr. Eng.*, vol. 72, pp. 191–202, Nov. 2018.
[37] M. Sharma and U. R. Acharya, "A new method to identify coronary artery disease with ECG signals and time-frequency concentrated antisymmetric biorthogonal wavelet filter bank," *Pattern Recognit. Lett.*, vol. 125, pp. 235–240, Jul. 2019.
[38] M. Sharma, A. V. Vanmali, and V. M. Gadre, "Construction of wavelets: Principles and practices," in *Wavelets and Fractals in Earth System Sciences*. Abingdon, U.K.: CRC Press, pp. 29–92, 2013.
[39] M. Sharma, R. Kolte, P. Patwardhan, and V. Gadre, "Time-frequency localization optimized biorthogonal wavelets," in *Proc. Int. Conf. Signal Process. Commun. (SPCOM)*, Jul. 2010, pp. 1–5.
[40] M. Sharma, D. Bhati, S. Pillai, R. B. Pachori, and V. M. Gadre, "Design of time-frequency localized filter banks: Transforming non-convex problem into convex via semidefinite relaxation technique," *Circuits, Syst., Signal Process.*, vol. 35, no. 10, pp. 3716–3733, Oct. 2016.
[41] Z. Luo, D. B. H. Tay, X. Lai, and Z. Lin, "Design of orthogonal wavelet filters with minimum RMS bandwidth using a symbolic approach," in *Proc. IEEE Int. Symp. Circuits Syst. (ISCAS)*, May 2021, pp. 1–5.
[42] M. Sharma, T. Singh, D. Bhati, and V. Gadre, "Design of two-channel linear phase biorthogonal wavelet filter banks via convex optimization," in *Proc. Int. Conf. Signal Process. Commun. (SPCOM)*, Jul. 2014, pp. 1–6.
[43] M. Sharma, V. M. Gadre, and S. Porwal, "An eigenfilter-based approach to the design of time-frequency localization optimized two-channel linear phase biorthogonal filter banks," *Circuits, Syst., Signal Process.*, vol. 34, no. 3, pp. 931–959, Mar. 2015.
[44] A. A. Bhurane, S. Dhok, M. Sharma, R. Yuvaraj, M. Murugappan, and U. R. Acharya, "Diagnosis of Parkinson's disease from electroencephalography signals using linear and self-similarity features," *Exp. Syst.*, vol. 39, no. 7, p. e12472, Aug. 2022.
[45] B. Hjorth, "EEG analysis based on time domain properties," *Electroencephalogr. Clin. Neurophysiol.*, vol. 29, no. 3, pp. 306–310, Sep. 1970.
[46] *MATLAB, Version 9.13.0.2049777 (R2022b)*. The MathWorks, Natick, MA, USA, 2022.
[47] B. Remeseiro and V. Bolon-Canedo, "A review of feature selection methods in medical applications," *Comput. Biol. Med.*, vol. 112, Sep. 2019, Art. no. 103375.
[48] Y. Nohara, K. Matsumoto, H. Soejima, and N. Nakashima, "Explanation of machine learning models using improved Shapley additive explanation," in *Proc. 10th ACM Int. Conf. Bioinf., Comput. Biol. Health Informat.*, Sep. 2019, p. 546.
[49] U. Bhatt, A. Xiang, S. Sharma, A. Weller, A. Taly, Y. Jia, J. Ghosh, R. Puri, J. M. F. Moura, and P. Eckersley, "Explainable machine learning in deployment," in *Proc. Conf. Fairness, Accountability, Transparency*, Jan. 2020, pp. 648–657.
[50] X. Geng, T.-Y. Liu, T. Qin, and H. Li, "Feature selection for ranking," in *Proc. 30th Annu. Int. ACM SIGIR Conf. Res. Develop. Inf. Retr.*, 2007, pp. 407–414.
[51] M. Sharma, V. Patel, J. Tiwari, and U. R. Acharya, "Automated characterization of cyclic alternating pattern using wavelet-based features and ensemble learning techniques with EEG signals," *Diagnostics*, vol. 11, no. 8, p. 1380, Jul. 2021.
[52] S. Dhok, V. Pimpalkhute, A. Chandurkar, A. A. Bhurane, M. Sharma, and U. R. Acharya, "Automated phase classification in cyclic alternating patterns in sleep stages using Wigner–Ville distribution based features," *Comput. Biol. Med.*, vol. 119, Apr. 2020, Art. no. 103691.
[53] F. Mendonca, A. Fred, S. S. Mostafa, F. Morgado-Dias, and A. G. Ravelo-Garcia, "Automatic detection of cyclic alternating pattern," *Neural Comput. Appl.*, vol. 34, pp. 1–11, 2018.
[54] H. W. Loh, C. P. Ooi, S. G. Dhok, M. Sharma, A. A. Bhurane, and U. R. Acharya, "Automated detection of cyclic alternating pattern and classification of sleep stages using deep neural network," *Int. J. Speech Technol.*, vol. 52, no. 3, pp. 2903–2917, Feb. 2022.
[55] M. Sharma, A. A. Bhurane, and U. R. Acharya, "An expert system for automated classification of phases in cyclic alternating patterns of sleep using optimal wavelet-based entropy features," *Exp. Syst.*, Feb. 2022, Art. no. e12939.
[56] F. Mendonça, S. S. Mostafa, F. Morgado-Dias, and A. G. Ravelo-García, "Matrix of lags: A tool for analysis of multiple dependent time series applied for CAP scoring," *Comput. Methods Programs Biomed.*, vol. 189, Jun. 2020, Art. no. 105314.
[57] S. Hartmann and M. Baumert, "Automatic A-phase detection of cyclic alternating patterns in sleep using dynamic temporal information," *IEEE Trans. Neural Syst. Rehabil. Eng.*, vol. 27, no. 9, pp. 1695–1703, Sep. 2019.
[58] M. O. Mendez, I. Chouvarda, A. Alba, A. M. Bianchi, A. Grassi, E. Arce-Santana, G. Milioli, M. G. Terzano, and L. Parrino, "Analysis of A-phase transitions during the cyclic alternating pattern under normal sleep," *Med. Biol. Eng. Comput.*, vol. 54, no. 1, pp. 133–148, 2016.
[59] S. Mariani, E. Manfredini, V. Rosso, M. O. Mendez, A. M. Bianchi, M. Matteucci, M. G. Terzano, S. Cerutti, and L. Parrino, "Characterization of a phases during the cyclic alternating pattern of sleep," *Clin. Neurophysiol.*, vol. 122, no. 10, pp. 2016–2024, Oct. 2011.
[60] F. Mendonça, S. S. Mostafa, A. Gupta, E. S. Arnardottir, T. Leppänen, F. Morgado-Dias, and A. G. Ravelo-García, "A-phase index: An alternative view for sleep stability analysis based on automatic detection of the A-phases from the cyclic alternating pattern," *Sleep*, vol. 46, no. 1, Jan. 2023, Art. no. zsac217.
[61] M. O. Mendez, A. Alba, I. Chouvarda, G. Milioli, A. Grassi, M. G. Terzano, and L. Parrino, "On separability of A-phases during the cyclic alternating pattern," in *Proc. 36th Annu. Int. Conf. IEEE Eng. Med. Biol. Soc.*, Aug. 2014, pp. 2253–2256.
[62] F. Machado, C. Teixeira, C. Santos, C. Bento, F. Sales, and A. Dourado, "A-phases subtype detection using different classification methods," in *Proc. 38th Annu. Int. Conf. IEEE Eng. Med. Biol. Soc. (EMBC)*, Aug. 2016, pp. 1026–1029.

MANISH SHARMA received the Ph.D. degree in electrical engineering from IIT, Bombay. He was a Postdoctoral Fellow with IIT, Indore, during 2016–2017. He is currently a Faculty Member with the Department of Electrical and Computer Science Engineering, IITRAM, Ahmedabad, India, an autonomous university established by the Government of Gujarat. He has more than 75 publications in reputed journals and conferences, of which 32 are H-indexed, and 50 are i-10 indexed (per Google Scholar, February 2022). His research interests include machine learning, healthcare data analytics, signal processing, and their applications. He received the "Excellence in the Ph.D. Research Work" (Best Ph.D. Thesis) Award for his outstanding research contributions from IIT, Bombay, in 2015. His research paper received the Honors Paper Award in recognition of outstanding work published in the SCI-indexed journal *Computers in Biology and Medicine*, in 2018. In June 2018, he received the "ERCIM" Alain Bensoussan Fellowship of the European Union for research from the Norwegian University of Science and Technology (NTNU), Norway. He has been listed in the world's top 2% of scientists in a study by Stanford University, USA, for three consecutive years (2019, 2020, and 2021).

HARSH LODHI is currently pursuing the Bachelor of Technology degree in electrical engineering with the Institute of Infrastructure, Technology, Research, and Management, Ahmedabad, India. His research interests include artificial intelligence, deep learning, computer-aided diagnosis, and data science.

RISHITA YADAV is currently pursuing the bachelor's degree in electrical engineering with the Institute of Infrastructure, Research, Technology, and Management (IITRAM), Ahmedabad. She has a minor in aerial robotics. Her research interests include pattern recognition, medical informatics, and AI for healthcare.

NIRANJANA SAMPATHILA (Senior Member, IEEE) received the B.E. degree in electronics and engineering and the M.Tech. degree in biomedical engineering from Mangalore University and the Ph.D. degree from Manipal University (currently known as the Manipal Academy of Higher Education, Manipal, India). He has more than 25 years of experience in research and academics in biomedical engineering applications. He is currently an Associate Professor-Senior Scale with the Manipal Institute of Technology, Manipal Academy of Higher Education. He has published a good number of papers in journals and conferences. His research interests include pattern recognition, medical informatics, miniaturized system design, nanoelectronics, and AI for healthcare. He is a Fellow of IE, India.

K. S. SWATHI received the B.A.M.S. degree from Kuvempu University, the M.B.A. degree in healthcare management, and the Ph.D. degree from the Manipal Academy of Higher Education, Manipal, India. She has more than 11 years of teaching experience in the area of healthcare management along with a short stint of experience in the hospital industry. She is currently an Associate Professor with the Prasanna School of Public Health, Manipal Academy of Higher Education. Her research interests include health services management, healthcare quality management, and health informatics.

U. RAJENDRA ACHARYA received the Ph.D., D.Eng., and D.Sc. degrees. He is currently a Professor with the University of Southern Queensland, Australia; a Distinguished Professor with the International Research Organization for Advanced Science and Technology, Kumamoto University, Japan; and an Adjunct Professor with the University of Malaya, Malaysia. His funded research has accrued cumulative grants exceeding six million Singapore dollars. He has authored over 500 publications, including 345 in refereed international journals, 42 in international conference proceedings, and 17 books. He has received more than 65,000 citations on Google Scholar (with an H-index of 128). His research interests include biomedical imaging and signal processing, data mining, and visualization, as well as applications of biophysics for better healthcare design and delivery. He is on the editorial boards of many journals and has served as the guest editor for several AI-related issues. He has been ranked in the top 1% of the highly cited researchers for the last seven consecutive years (2016–2022) in computer science, according to the Essential Science Indicators of Thomson.